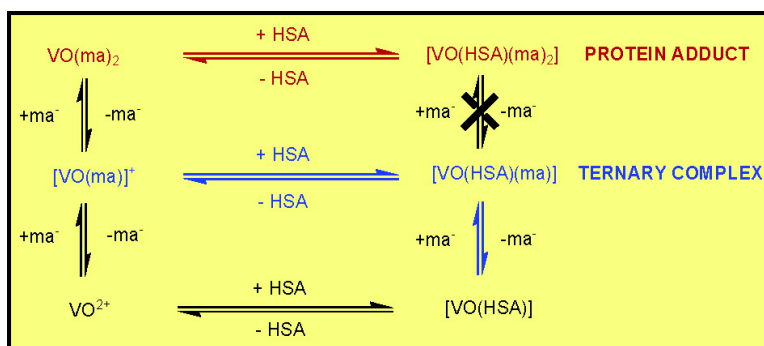


## New Insights into the Interactions of Serum Proteins with Bis(maltolato)oxovanadium(IV): Transport and Biotransformation of Insulin-Enhancing Vanadium Pharmaceuticals

Barry D. Liboiron, Katherine H. Thompson, Graeme R. Hanson, Edmond Lam, Nicolas Aebischer, and Chris Orvig

*J. Am. Chem. Soc.*, **2005**, 127 (14), 5104-5115 • DOI: 10.1021/ja043944n • Publication Date (Web): 19 March 2005

Downloaded from <http://pubs.acs.org> on March 25, 2009



### More About This Article

Additional resources and features associated with this article are available within the HTML version:

- Supporting Information
- Links to the 2 articles that cite this article, as of the time of this article download
- Access to high resolution figures
- Links to articles and content related to this article
- Copyright permission to reproduce figures and/or text from this article

[View the Full Text HTML](#)



## New Insights into the Interactions of Serum Proteins with Bis(maltolato)oxovanadium(IV): Transport and Biotransformation of Insulin-Enhancing Vanadium Pharmaceuticals

Barry D. Liboiron,<sup>†,§</sup> Katherine H. Thompson,<sup>†</sup> Graeme R. Hanson,<sup>\*,‡</sup>  
Edmond Lam,<sup>†,||</sup> Nicolas Aebischer,<sup>†,⊥</sup> and Chris Orvig<sup>\*,†</sup>

Contribution from the Department of Chemistry, University of British Columbia,  
2036 Main Mall, Vancouver, BC, Canada, V6T 1Z1, and Centre for Magnetic Resonance,  
University of Queensland, St. Lucia, Queensland, Australia, 4072

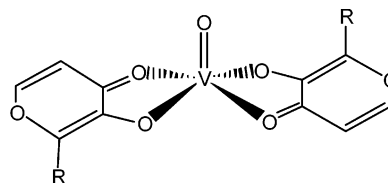
Received October 5, 2004; E-mail: orvig@chem.ubc.ca; graeme.hanson@cmr.uq.edu.au

**Abstract:** Significant new insights into the interactions of the potent insulin-enhancing compound bis(maltolato)oxovanadium(IV) (BMOV) with the serum proteins, apo-transferrin and albumin, are presented. Identical reaction products are observed by electron paramagnetic resonance (EPR) with either BMOV or vanadyl sulfate (VOSO<sub>4</sub>) in solutions of human serum apo-transferrin. Further detailed study rules out the presence of a ternary ligand-vanadyl-transferrin complex proposed previously. By contrast, differences in reaction products are observed for the interactions of BMOV and VOSO<sub>4</sub> with human serum albumin (HSA), wherein adduct formation between albumin and BMOV is detected. In BMOV–albumin solutions, vanadyl ions are bound in a unique manner not observed in comparable solutions of VOSO<sub>4</sub> and albumin. Presentation of chelated vanadyl ions precludes binding at the numerous nonspecific sites and produces a unique EPR spectrum which is assigned to a BMOV–HSA adduct. The adduct species cannot be produced, however, from a solution of VOSO<sub>4</sub> and HSA titrated with maltol. Addition of maltol to a VOSO<sub>4</sub>–HSA solution instead results in formation of a different end product which has been assigned as a ternary complex, VO(ma)(HSA). Furthermore, analysis of solution equilibria using a model system of BMOV with 1-methylimidazole (formation constant  $\log K_1 = 4.5(1)$ , by difference electronic absorption spectroscopy) lends support to an adduct binding mode (VO(ma)<sub>2</sub>–HSA) proposed herein for BMOV and HSA. This detailed report of an in vitro reactivity difference between VOSO<sub>4</sub> and BMOV may have bearing on the form of active vanadium metabolites delivered to target tissues. Albumin binding of vanadium chelates is seen to have a potentially dramatic effect on pharmacokinetics, transport, and efficacy of these antidiabetic chelates.

### Introduction

Vanadium complexes have shown considerable promise as an orally available treatment for diabetes mellitus. Bis(maltolato)oxovanadium(IV) (BMOV) is one of a number of complexes that have demonstrated superior activity over inorganic vanadium sources (e.g., VOSO<sub>4</sub> or NaVO<sub>3</sub>) through both in vivo and/or in vitro assays of biological effectiveness.<sup>1–3</sup> Short-term administration of inorganic vanadium to Type II diabetic patients

has resulted in significant amelioration of diabetes symptomatology in several studies.<sup>4–7</sup> BEOV, a closely related analogue to BMOV, recently completed Phase I clinical trials to evaluate its use as a pharmaceutical agent for the treatment of Type II diabetes mellitus.



R = CH<sub>3</sub>, Bis(maltolato)oxovanadium(IV), BMOV  
R = C<sub>2</sub>H<sub>5</sub>, Bis(ethylmaltolato)oxovanadium(IV), BEOV

Neither the mechanism nor the metabolic fate of vanadium compounds is well understood. Vanadium, whether administered

<sup>†</sup> University of British Columbia.

<sup>‡</sup> University of Queensland.

<sup>§</sup> Current address: Department of Chemistry, Stanford University, Stanford, California, 94305.

<sup>||</sup> Current address: Department of Chemistry, University of Toronto, 80 St. George Street, Toronto, Ontario M5S 3H6.

<sup>⊥</sup> Current address: Vifor SA, Fribourg, Switzerland.

(1) Thompson, K. H.; McNeill, J. H.; Orvig, C. *Chem. Rev.* **1999**, *99*, 2561–2571.

(2) Shechter, Y.; Eldberg, G.; Shisheva, A.; Gefel, D.; Sekar, N.; Qian, S.; Bruck, R.; Gershonov, E.; Crans, D. C.; Goldwasser, Y.; Fridkin, M.; Li, J. In *Vanadium Compounds: Chemistry, Biochemistry, and Therapeutic Applications*; Tracey, A. S., Crans, D. C., Eds.; American Chemical Society: Washington, D.C., 1998; Vol. 711, pp 308–315.

(3) Yuen, V. G.; Orvig, C.; McNeill, J. H. *Can. J. Physiol. Pharmacol.* **1993**, *71*, 263–269.

(4) Cohen, N.; Halberstam, M.; Shlimovich, P.; Chang, C. J.; Shamoan, H.; Rossetti, L. *J. Clin. Invest.* **1995**, *95*, 2501–2509.

(5) Boden, G.; Chen, X.; Ruiz, J.; Rossum, G. D. V.; Turco, S. *Metabolism* **1996**, *45*, 1130–1135.

as a vanadium salt or a chelated source such as BMOV, accumulates predominately in bone, liver, and kidney tissue.<sup>8–12</sup> Both the amount and relative vanadium concentrations in these organs vary with the particular compound and dose, but the amount is generally significantly higher from chelated sources.<sup>12–14</sup> The greater pharmacological effect of BMOV compared to that of  $\text{VOSO}_4$  was attributed provisionally to increased absorption from the gastrointestinal tract due to the low molecular weight, acceptable lipophilic/hydrophilic balance, and neutral charge of the vanadyl complex.<sup>3,15</sup> Increased absorption as a possible mechanism was supported by a kinetic analysis comparing  $^{48}\text{V}$ -labeled compounds<sup>12</sup> and by a cellular model of intestinal absorption, in which vanadium uptake from BMOV was nearly double that from  $\text{VOSO}_4$ .<sup>13</sup> This interpretation was also supported by our recent studies which showed that the  $^{14}\text{C}$ -labeled ligand and the vanadium from bis(1- $^{14}\text{C}$ -ethylmaltolato)oxovanadium(IV) (1- $^{14}\text{C}$ -BEOV) cleared the bloodstream in a kinetically dissimilar fashion.<sup>14</sup> The calculated pharmacokinetic parameters for vanadium and  $^{14}\text{C}$  strongly supported the hypothesis of rapid (<1 h) dissociation following an oral dose of BEOV.<sup>3,14,15</sup>

Absorption enhancement does not necessarily explain all of the relevant findings, however. For example, either a small amount of intact complex could be responsible for the antidiabetic effect or the complex could act as a prodrug to augment the delivery of an active vanadium metabolite (as yet undetected) to a target tissue. With regard to how small an amount might be relevant to in vivo antidiabetic efficacy, it is worth noting that oral antidiabetic efficacy of  $\text{VOSO}_4$  is presumably attributable to the 1–5% of a dose that is absorbed.<sup>15,16</sup> If all of the complex completely dissociated at the level of absorption, one might expect no difference in biodistribution between chelated and inorganic vanadyl sources, contrary to observation.<sup>12,17,18</sup> Significant differences in organ accumulation depending on chelation of vanadium have, in fact, been observed, with chelation generally resulting in two to four times higher tissue vanadium concentration compared to inorganic vanadium sources.<sup>12,13,18,19</sup> In a direct comparison between several chelated vanadyl sources, differences were noted between complexes in how much vanadium arrived at potential target tissues, notably liver and muscle. In bone, the most significant accumulator of vanadium, 0.2 to 0.3  $\mu\text{mol V/g}$  bone was measured after 2 to 12 weeks of chelated vanadyl complex supplementation at a

dose relevant to diabetes therapy;<sup>13,18</sup> however, vanadium levels usually decline rapidly once supplementation is discontinued.<sup>20</sup>

In addition, most in vitro studies comparing vanadium chelates to inorganic vanadium compounds demonstrate enhancement of insulin-like effects at the cellular level. Relative rankings from these findings are not entirely consistent with in vivo comparisons;<sup>14,18</sup> nonetheless, chelated V(IV) complexes are generally more effective than  $\text{VOSO}_4$  in vitro,<sup>21</sup> lending credence to a role for complexation at a postabsorptive level. A pharmacological benefit of vanadyl chelation beyond absorption, with a small portion of the administered complex remaining intact after absorption, could contribute to the differences in biodistribution and efficacy that are seen.<sup>18,21</sup>

If the greater efficacy of BMOV compared to that of  $\text{VOSO}_4$  is at least partly due to ligand effects at the level of the systemic circulation or beyond, to what might this be attributable? Two serum proteins implicated in the transport of vanadium ions (both V(IV) and V(V)) are apo-transferrin (apo-Tf) and human serum albumin (HSA). Elucidation of differences in transport between BMOV and  $\text{VOSO}_4$  are most likely to be relevant to this question.

Apo-transferrin (apo-Tf), a bilobal single chain protein, is the main Fe(III) transport protein in serum. It is capable of tight reversible binding of two equivalents of Fe(III) and has been shown to bind a wide variety of other metal ions such as group 13 ions,<sup>22,23</sup> vanadyl,<sup>24</sup> and several lanthanide ions.<sup>25–28</sup> Apo-Tf binds 2 equiv of  $\text{VO}^{2+}$  at the Fe(III) sites,<sup>29</sup> and this binding requires a synergistic binding anion.<sup>24</sup> Vanadyl ion binding occurs in up to three different conformations (termed A, B<sub>1</sub>, and B<sub>2</sub>), which are EPR (Q-band) detectable.<sup>30</sup> Human serum albumin (HSA), the most prevalent protein in the blood (0.65 mM),<sup>31</sup> is a large globular protein with several physiological roles ranging from transport of hydrophobic metabolites such as fatty acids to Cu(II) and Zn(II) transport<sup>31</sup> and the maintenance of blood osmotic pressure.<sup>32</sup> Albumin binds 1 equiv of  $\text{VO}^{2+}$  in the Cu(II) site at the N-terminus, likely through the H3 imidazole (the “strong” site) and several equivalents via nonspecific interactions with carboxylate side chains of surface amino acids (“weak” sites).<sup>33</sup> The exact number of possible nonspecific  $\text{VO}^{2+}$  binding sites is at least five,<sup>33</sup> and possibly as many as twenty.<sup>32</sup>

In this work, we report extended studies of the interactions of BMOV and  $\text{VOSO}_4$  with the two serum proteins, apo-Tf and HSA. In the case of apo-Tf, no discernible differences exist in the reactivities of BMOV versus  $\text{VOSO}_4$ , while, for HSA, the formation of a BMOV–HSA adduct may represent an important

- (6) Goldfine, A. B.; Patti, M.-E.; Zuberi, L.; Goldstein, B. J.; LeBlanc, R.; Landaker, E. J.; Jiang, Z. Y.; Willsky, G. R.; Kahn, C. R. *Metabolism* **2000**, *49*, 400–410.
- (7) Cusi, K.; Cukier, S.; DeFronzo, R. A.; Torres, M.; Puchulu, F. M.; Redondo, J. C. *J. Clin. Endocrinol. Metab.* **2001**, *86*, 1410–1417.
- (8) Hopkins, L. L., Jr.; Tilton, B. E. *Am. J. Physiol.* **1966**, *211*, 169–172.
- (9) Parker, R. D. R.; Sharma, R. P. *J. Environ. Pathol. Toxicol.* **1978**, *2*, 235–245.
- (10) Wiegmann, T. B.; Day, H. D.; Patak, R. V. *J. Toxicol. Environ. Health* **1982**, *10*, 233–245.
- (11) Al-Bayati, M.; Raabe, O. G.; Giri, S. N.; Knaak, J. B. *J. Am. Coll. Toxicol.* **1991**, *10*, 233–241.
- (12) Setyawati, I. A. et al. *J. Appl. Physiol.* **1998**, *84*, 569–575.
- (13) Thompson, K. H.; Tsukada, Y.; Xu, Z.; Battell, M.; McNeill, J. H.; Orvig, C. *Biol. Trace Elem. Res.* **2002**, *86*, 31–44.
- (14) Thompson, K. H. et al. *J. Biol. Inorg. Chem.* **2003**, *8*, 66–74.
- (15) Thompson, K. H.; Orvig, C. *J. Chem. Soc., Dalton Trans.* **2000**, 2885–2892.
- (16) Nielsen, F. H. In *Metal Ions in Biological Systems*; Sigel, H., Sigel, A., Eds.; Marcel Dekker: New York, 1995; Vol. 31, pp 543–573.
- (17) Makinen, M. W.; Brady, M. J. *J. Biol. Chem.* **2002**, *277*, 12215–12220.
- (18) Takino, T.; Yasui, H.; Yoshitake, A.; Hamajima, Y.; Matsushita, R.; Takada, J.; Sakurai, H. *J. Biol. Inorg. Chem.* **2001**, *6*, 133–142.
- (19) Reul, B. A.; Amin, S. S.; Buchet, J.-P.; Ongemba, L. N.; Crans, D. C.; Brichard, S. M. *Br. J. Pharmacol.* **1999**, *126*, 467–477.

- (20) Thompson, K. H.; Battell, M.; McNeill, J. H. In *Vanadium in the Environment. Part 2. Health Effects*; Nriagu, J. O., Ed.; John Wiley and Sons: New York, 1998; Vol. 31, pp 21–37.
- (21) Rehder, D.; Pessoa, J. C.; Geraldes, C. F. G. C.; Castro, M. M. C. A.; Kabanos, T.; Kiss, T.; Meier, B.; Micera, G.; Pettersson, L.; Rangel, M.; Salifoglou, A.; Turel, I.; Wang, D. *J. Biol. Inorg. Chem.* **2002**, *7*, 384–396.
- (22) Harris, W. R.; Pecoraro, V. L. *Biochemistry* **1983**, *22*, 292–299.
- (23) Harris, W. R.; Sheldon, J. *Inorg. Chem.* **1990**, *29*, 119–124.
- (24) Campbell, R.; Chasteen, N. D. *J. Biol. Chem.* **1977**, *252*, 5996–6001.
- (25) Harris, W. R. *Inorg. Chem.* **1986**, *25*, 2041–2045.
- (26) Harris, W. R.; Chen, Y. *Inorg. Chem.* **1992**, *31*, 5001–5006.
- (27) Taylor, D. M.; Duffield, J. R.; Williams, D. R.; Yule, L.; Gaskin, P. W.; Unal, P. *Eur. J. Sol. State Inorg. Chem.* **1991**, *28*, 271–274.
- (28) Zak, O.; Aisen, P. *Biochemistry* **1988**, *27*, 1075–1080.
- (29) Cannon, J. C.; Chasteen, N. D. *Biochemistry* **1975**, *14*, 4573–4577.
- (30) White, L. K.; Chasteen, N. D. *J. Phys. Chem.* **1979**, *83*, 279–283.
- (31) Sarkar, B. *Biol. Trace Elem. Res.* **1989**, *21*, 1075–1080.
- (32) Purcell, M.; Neault, J. F.; Malonga, H.; Arakawa, H.; Tajmir-Riahi, H. A. *Can. J. Chem.* **2001**, *79*, 1415–1421.
- (33) Chasteen, N. D.; Francavilla, J. *J. Phys. Chem.* **1976**, *80*, 867–871.

difference in serum interactions between chelated vanadyl and an inorganic vanadyl source. Through detailed analysis of EPR spectra, we propose the formation of a unique BMOV–HSA adduct complex that is spectroscopically distinct from the vanadyl–HSA complex formed with  $\text{VO}_4$  or the ternary ma-VO–HSA species found by adding maltol to the latter. The formation of the BMOV–HSA adduct complex is supported by titrations of BMOV with 1-methylimidazole (ImMe). These studies determined that the formation of the BMOV–ImMe adduct is thermodynamically favored, offering a potential method by which BMOV–albumin adducts could form in vivo.

## Materials and Methods

**Materials.** Water was distilled (Corning MP-1 Megapure still) and deionized (Barnstead D9802 and D9804 cartridges) prior to use. Human serum apo-transferrin and human serum albumin were obtained from Sigma-Aldrich. Apo-transferrin was 97% iron-free and obtained as a lyophilized powder (Sigma #T4283). Albumin (98%) was globulin-free, crystallized, and lyophilized (Sigma #A8762). Sodium carbonate, vanadyl sulfate trihydrate, sodium chloride, citric acid, 1-methylimidazole, 1,10-phenanthroline, and 4-(2-hydroxyethyl)-1-piperazineethane sulfonic acid (HEPES) were of the highest grade available from Sigma-Aldrich and were used as received. Atomic absorption standard (AAS) solutions of vanadium and iron were obtained from Aldrich. Maltol (Hma) was obtained from Pfizer. BMOV was synthesized according to established procedures.<sup>34</sup> The structure and purity of BMOV was confirmed by Fourier transform infrared spectroscopy, mass spectrometry (liquid secondary ion ionization, positive detection), and elemental analysis.

**Solution Preparation.** To avoid adventitious metal ion binding, glassware was demetalated prior to use. Glassware, sample tubes, and storage tubes were either placed in a 1 M  $\text{HNO}_3$  bath for extended periods or thoroughly rinsed with Chelex-100 resin (Aldrich) in  $\text{H}_2\text{O}$ . All solutions were made from reagent grade materials. All bulk dialysis solutions and buffers were stored over  $\sim 20$  mL of Chelex-100 resin in  $\text{H}_2\text{O}$ . All pH readings were obtained with a Metrohm glass combination electrode interfaced with a Fisher potentiometer, previously calibrated against pH 4.0 and pH 7.0 standard buffer solutions (Aldrich). Unless otherwise stated, all solutions were prepared in 0.05 M HEPES buffer at pH 7.4. EPR spectra of BMOV in water and in the above buffer were identical, indicating negligible binding of buffer ions to the BMOV complex.

**Protein Purification and Manipulation.** Both proteins were dialyzed using Sigma cellulose dialysis tubing with a molecular weight exclusion limit of 10 kDa, based on methods previously reported by Harris and Pecoraro (apo-Tf)<sup>22</sup> and Chasteen and Francavilla (HSA).<sup>33</sup> Concentrations of apo-Tf were determined by spectrophotometric titration ( $\lambda = 253$  nm) against a carefully prepared 1:3 solution of  $\text{FeCl}_3$  and nitrilotriacetic acid (pH 4.0). The titration was monitored by a HP8453 diode array UV–vis spectrophotometer, and the concentration was determined by the interception point of the two linear regions of an absorbance versus equivalents Fe(III) plot. The concentration of HSA was determined spectrophotometrically ( $\lambda = 278$  nm;  $\epsilon = 4.2 \times 10^4 \text{ M}^{-1} \text{ cm}^{-1}$ ).<sup>35</sup> Both proteins were concentrated using a SpeedVac concentrator.

**General Procedure for Preparation of Protein Samples.** Oxidation of V(IV) to V(V) species was prevented through the use of anaerobic protocols throughout all preparative procedures. Pure Ar (99.8%) was humidified by passage through a gas dispersion tube into a volume of degassed water before introduction into reaction vessels where volumetric amounts were required. Degassing of all protein solutions was achieved by a gentle flow of Ar over the surface of the solution for

30–40 min prior to sample manipulations. Degassing of analytical solutions (e.g., buffers, BMOV, ligand) was completed by Ar sparge in a septum-sealed vessel for at least 1 h. For samples prepared for low temperature study, glycerol was added as a cryoprotectant to ensure good glass formation. Glycerol concentration was set at either 33 or 50 vol %.

**Preparation of Carbonate-Free Apo-Transferrin Solution.** The method used was based upon an earlier procedure developed by Campbell and Chasteen.<sup>24</sup> Apo-Tf, in a solution of 0.05 M HEPES buffer (pH 7.4), was placed in a septum-sealed three-neck pear-shaped flask equipped with a combination glass electrode for pH measurement. The solution was acidified, dropwise by syringe, with 1 M HCl to pH 3.5 with gentle stirring.  $\text{CO}_2$ -free (passed through 40% w/v NaOH scrubbing solution) and humidified (preboiled  $\text{H}_2\text{O}$ ) Ar was passed over the surface of the solution for 40 min. The pH was returned to 7.4 by blowing  $\text{NH}_3$  gas over the solution surface. Ammonia, in a carrier Ar gas described above, was generated by bubbling scrubbed Ar through a 1:1 solution of 25% w/v NaOH and concentrated aqueous ammonium hydroxide.

**Stability of the (1-Methylimidazole)–BMOV Adduct.** The general procedure for titration of BMOV with 1-methylimidazole (ImMe) follows. A stock BMOV solution was made using degassed 0.05 M HEPES buffer with 0.16 M NaCl, pH 7.4. An aliquot of the stock solution was diluted to the desired concentration with additional buffer, in Ar-purged flasks. This dilute BMOV solution served as the analytical solution for the titration. A titrant solution of ImMe (MW = 82.10 g  $\text{mol}^{-1}$ ,  $\rho = 1.03 \text{ g mL}^{-1}$ ) was prepared in degassed 0.05 M HEPES buffer with 0.16 M NaCl, pH 7.4. The titration of the analytical solution by the ImMe solution was monitored at 275 nm by withdrawing, by syringe, aliquots of the sample solution during the experiment. Aliquots were returned to the reaction solution after measurement. Electronic absorption measurements were conducted at 298 K, after a 15 min equilibration period. Absorbance data were corrected for dilution effects. Experimental data were fitted by a nonlinear least squares curve fitting routine within SigmaPlot 2001 (SPSS, Inc.). The concentration of each analyte at a given experimental point was determined relative to that of the BMOV–ImMe adduct (eq 1), which in turn were used to generate theoretical absorbances for each experimental value (eq 2). The differences were minimized by iteration of the extinction coefficient of the adduct and the formation constant of BMOV–ImMe.

$$[\text{BMOV–ImMe}] = \frac{-(K_1 B_T + K_1 I_T + 1) \pm \sqrt{(K_1 B_T + K_1 I_T + 1)^2 - 4K_1^2 B_T I_T}}{-2K_1} \quad (1)$$

where  $K_1$  is the equilibrium constant for adduct formation,  $B_T$ , the total concentration of all BMOV species, and  $I_T$ , the total concentration of all ImMe species.

$$A = \epsilon_{\text{BMOV}}[\text{BMOV}] + \epsilon_{\text{ImMe}}[\text{ImMe}] + \epsilon_1[\text{BMOV–ImMe}] \quad (2)$$

The extinction coefficient for BMOV was determined using a Beer's Law plot. For the adduct, the absorbances of solutions of BMOV with a 25 molar excess of ImMe were used to produce the Beer's Law plot. Experimental extinction coefficients used in the iterative curve fitting were:  $\epsilon_{275}(\text{BMOV}) = (14.3 \pm 0.3) \times 10^3 \text{ M}^{-1} \text{ cm}^{-1}$ ;  $\epsilon_{275}(\text{BMOV–ImMe}) = (17.3 \pm 0.7) \times 10^3 \text{ M}^{-1} \text{ cm}^{-1}$ ;  $\epsilon_{275}(\text{ImMe}) < 3 \text{ M}^{-1} \text{ cm}^{-1}$ .

**EPR Spectroscopy.** EPR spectra were acquired on two instruments. Most spectra were acquired on a Bruker ECS-106 X-band spectrometer (Department of Chemistry, University of British Columbia), equipped with an EIP 562A microwave frequency counter and a Varian E500 gaussmeter for the calibration of the microwave frequency and magnetic field, respectively. Spectra were recorded in a  $\text{TM}_{011}$  cavity. Some X-band experiments were conducted on a Bruker Elexsys E500 spectrometer (Centre for Magnetic Resonance, University of Queensland) equipped with an EIP 548B frequency counter, Bruker ER 035M

(34) Caravan, P. et al. *J. Am. Chem. Soc.* **1995**, *117*, 12759–12770.

(35) Reynolds, J. A.; Gallagher, J. P.; Steinhardt, J. *Biochemistry* **1970**, *9*, 1232–1238.



NMR gaussmeter, and a Bruker super high Q cavity. For both instruments, variable temperature (100–298 K) regulation was achieved through the use of a liquid nitrogen flow-through cryostat coupled with a Eurotherm B-VT-2000 temperature controller. Typical acquisition parameters were as follows: power 0.2 (low temperature) to 50 (room temperature) mW; modulation amplitude 1 to 5.1 G; sweep time 84 s; 2048 or 4096 points. Before normalizing the EPR spectra presented herein to a common microwave frequency, we checked that the changes in resonant field positions as a consequence of *g*-strain broadening (a frequency-dependent line width effect) were negligible.

Computer simulation of the EPR spectra was performed using version 1.1.3 of the XSophe-Sophe-XeprView computer simulation software suite, running on a personal computer with the Mandrake Linux operating system (v9.1).<sup>36–38</sup> The computational program, SOPHE, employs a number of methods, including matrix diagonalization, SOPHE interpolation, and homotopy for the analysis of randomly oriented EPR spectra. In this research we employed matrix diagonalization in conjunction with mosaic misorientation to simulate the randomly oriented EPR spectra. This method significantly reduces the computational times. Comparisons of simulated and experimental spectra and data manipulation were performed with Xepr (Bruker, v 1.2), WinEPR (Bruker Biospin), and/or SigmaPlot 2001 (SPSS, Inc.). For Gaussian fitting of EPR peak intensities, PeakFit v4 (SPSS, Inc.) was used.

## Results

Low molecular weight  $\text{VO}^{2+}$  complexes such as BMOV yield nearly isotropic EPR spectra, analogous to those observed for the vanadyl ion<sup>39</sup> in acidic solutions. At higher pH values (e.g., pH 7.4 as in this study) uncoordinated  $\text{VO}^{2+}$  ions form an EPR-silent hydroxo-bridged dimer,<sup>33,39</sup> thus unbound vanadyl ions make no contribution to the EPR spectrum at the pH used in these studies. Binding of the small vanadyl ion to large protein molecules is observed at room temperature as highly anisotropic (slow motion regime) spectra. In contrast, nearly isotropic (motionally averaged) spectra are obtained for the vanadyl ion (i.e.,  $[\text{VO}(\text{H}_2\text{O})_5]^{2+}$ ) in acidic solution<sup>39</sup> as well as for small complexes such as BMOV at ambient pH values.<sup>34</sup> Thus room temperature EPR spectroscopy is a useful probe for the detection of protein bound vanadyl moieties. Characterization and quantification of the detected species can then be carried out using frozen solution (rigid limit) EPR spectroscopy.

The differences between the solution spectra of the low molecular weight BMOV complex (Figure 1e) and the VO–protein reaction products (VO–Tf, Figure 1a; BMOV–Tf, Figure 1b) are prominent.

Clearly, BMOV and apo-Tf react to form a vanadyl–protein complex, and through comparison with the  $\text{VOSO}_4$  spectrum (Figure 1a), it is apparent that this reaction results in a similar, if not identical, species to that obtained with  $\text{VOSO}_4$  as the source of vanadyl ions. Beyond addition of 2 equiv of BMOV, the nearly isotropic spectrum of free BMOV becomes prominent in the room temperature spectrum (data not shown). These spectra indicate that either the BMOV–Tf complex has an identical EPR spectrum to that of  $(\text{VO})_x\text{-Tf}$  (where  $x = 1, 2$ ) (highly unlikely) or that apo-Tf extracts the metal ion from the BMOV complex (quite possible) to form the previously characterized  $(\text{VO})_x\text{-Tf}$  complex.

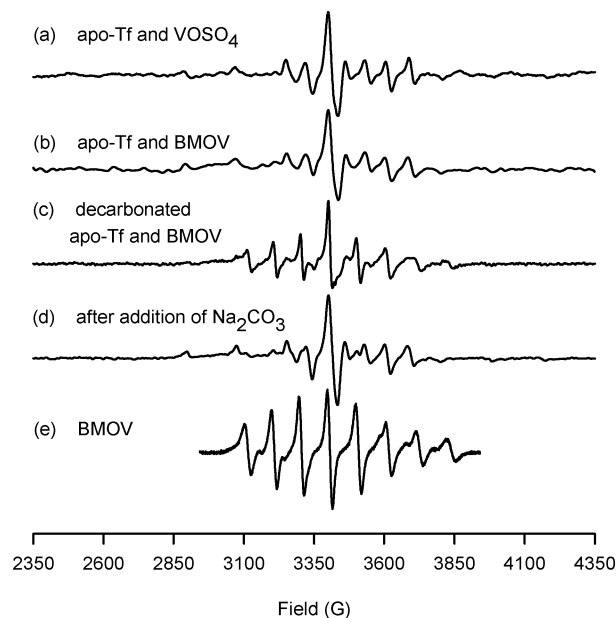


**Figure 1.** Room temperature EPR spectra of (a) [apo-Tf] = 0.29 mM and  $[\text{VOSO}_4] = 1.11$  mM, ambient  $[\text{HCO}_3^-]$ ; (b) [apo-Tf] = 0.134 mM and  $[\text{BMOV}] = 0.112$  mM, ambient  $[\text{HCO}_3^-]$ ; (c) decarbonated apo-Tf and BMOV; (d) after addition of excess  $\text{Na}_2\text{CO}_3$ ; (e)  $[\text{BMOV}] = 1.10$  mM ( $T = 298$  K, pH 7.4, 0.16 M NaCl,  $\nu = 9.5794$  GHz).

Vanadyl sulfate was previously shown to require a synergistic binding anion, such as bicarbonate, or others which have also been shown to be active in Fe(III) binding.<sup>22,24</sup> Active synergistic anions possess a carboxylic acid functionality, a second potential donor atom one or two carbons away from the carboxylate and a negative or dinegative charge.<sup>24</sup> While maltolate does not possess all of these attributes, it has been postulated that different reaction products could be produced if one of the maltolato ligands of BMOV were acting as the synergistic anion, replacing bicarbonate.<sup>40</sup>

Careful exclusion and elimination of ambient bicarbonate demonstrates that BMOV does not interact with apo-Tf in its absence. The EPR spectrum of a decarbonated BMOV/apo-Tf solution (Figure 1c) is largely isotropic with only a small anisotropic contribution. While the isotropic component corresponds to “free” BMOV (cf. Figure 1e), the small anisotropic component  $(\text{VO})_x\text{-Tf}$  arises from the presence of a small amount of residual bicarbonate that remains in solution after the decarbonation procedure ( $\sim 10\%$  of the ambient concentration is expected from Campbell et al.<sup>24</sup>) which allows for formation of a corresponding amount of  $(\text{VO})_x\text{-Tf}$ . Addition of a synergistic anion (sodium carbonate) to the decarbonated BMOV/apo-Tf solution produces the same BMOV–Tf EPR spectrum shown earlier (Figure 1d, cf. Figure 1b). Thus, maltolate cannot substitute for bicarbonate and facilitate coordination of BMOV to apo-Tf via a ternary complex, and the presence of a synergistic anion such as (bi)carbonate is required for BMOV-sourced vanadyl ions to bind to apo-Tf. This result is consistent with an earlier study that demonstrated that active synergistic anions all possessed a uni- or dinegative charge as well as the presence of a carbonyl oxygen on the same carbon possessing a negative charge.<sup>24</sup> This result also suggests that loss of at least one maltol ligand is required for BMOV binding

(36) Wang, D.; Hanson, G. R. *J. Magn. Reson.* **1995**, *177*, 1–8.  
 (37) Griffin, M.; Muys, A.; Noble, C.; Wang, D.; Eldershaw, C.; Gates, K. E.; Burrage, K.; Hanson, G. R. *Mol. Phys. Rep.* **1999**, *26*, 60–84.  
 (38) Hanson, G. R.; Gates, K. E.; Noble, C. J.; Griffin, M.; Michell, A.; Benson, S. *J. Inorg. Biochem.* **2004**, *98*, 903–916.  
 (39) Chasteen, N. D. *Biol. Magn. Reson.* **1981**, *3*, 53–119.

(40) Willsky, G. R.; Goldfine, A. B.; Kostyniak, P. J.; McNeill, J. H.; Yang, L. Q.; Khan, H. R.; Crans, D. C. *J. Inorg. Biochem.* **2001**, *85*, 33–42.

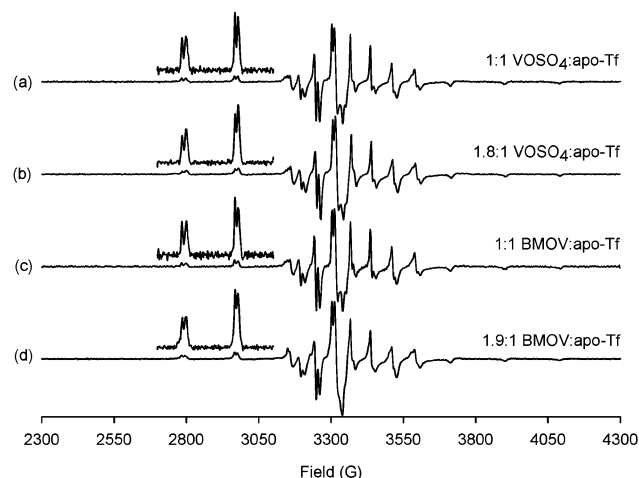


**Figure 2.** EPR spectra of  $(VO)_2^+$ -transferrin ( $T = 130$  K, pH 7.40, 0.16 M NaCl,  $\nu = 9.3468$  GHz); (a)  $[VOSO_4]/[apo-Tf] = 0.9$ ; (b)  $[VOSO_4]/[apo-Tf] = 1.8$ ; (c)  $[BMOV]/[apo-Tf] = 0.85$ ; (d)  $[BMOV]/[apo-Tf] = 1.9$ . Insets: expansion of the  $-7/2_{||}$  (downfield) and  $-5/2_{||}$  (upfield) resonances.

to apo-Tf in order to accommodate synergistic binding of (bi)carbonate.

Vanadyl ions have been shown to bind specifically in the Fe(III) sites,<sup>29</sup> and EPR can be used to demonstrate that BMOV-sourced  $VO^{2+}$  ions bind in the same sites. Addition of Fe(III) to a solution of BMOV and apo-Tf transformed the observed anisotropic spectrum to that of BMOV (see Supporting Information, Figure S1). Thus, Fe(III) displaces  $VO^{2+}$  ions from the protein, regardless of the vanadyl source. The displacement is not quantitative under the conditions of Figure S1, a consequence of the presence of free maltol (lending further support to our conclusion that BMOV is decomposed by apo-Tf), which competes effectively for Fe(III) through the formation of the highly stable tris complex,  $Fe(ma)_3$  ( $\log \beta_3 = 28.45$ ).<sup>41</sup> Secondly, rapid addition of Fe(III) to a solution at pH 7.4 probably results in some hydrolysis to ferric hydroxide, due to the very strong hydrolysis reactions of Fe(III) and subsequent slow conversion to soluble Fe complexes in the presence of chelating ligands. Upon addition of excess equivalents of Fe(III), virtually all of the vanadyl ions are displaced and re-form BMOV.

Frozen solution EPR spectra of apo-Tf with BMOV or  $VOSO_4$  in 1:1 and 2:1 ratios are presented in Figure 2. The four spectra are virtually superimposable. Examination of the low field parallel region of each spectrum reveals that two distinct sets of resonances comprise each spectrum, which were previously detected and assigned as different VO-protein conformations (downfield signal as B and upfield signal as A conformations, see Table 1 for field values) by Chasteen and co-workers.<sup>29</sup> The B signal is not split into  $B_1$  and  $B_2$  conformations, as was observed in an earlier Q-band (35 GHz) EPR study.<sup>30</sup> The spectra of 1:1 and 2:1 solutions of either  $VOSO_4$  or BMOV with apo-Tf clearly demonstrate that both vanadyl sources bind in both conformations. A careful examination of these peaks reveals slight intensity differences (by peak height) which we studied by calculating the relative area of the  $-7/2_{||}$  (at 2790 G) and  $-5/2_{||}$  peaks (at 2975 G) of each conformation for each vanadyl source. The relative intensities of the overlapping peaks in the low field parallel region were

**Table 1.** Parameters Derived from Gaussian Fitting of  $-5/2_{||}$  Peaks of EPR Spectra of  $VOSO_4$  or BMOV with Apo-Tf<sup>a</sup>

sample	resonant field (G)		peak width <sup>b</sup> (G)		relative peak area <sup>c</sup> (%)
	B	A	B	A	
1:1 $VOSO_4$ /Tf	2967.7 (0.3)	2979.5 (0.2)	6.3	11.3	63.5 (5.0)
2:1 $VOSO_4$ /Tf	2968.0 (0.3)	2979.6 (0.3)	6.4	10.2	52.5 (2.1)
1:1 BMOV/Tf	2968.0 (0.4)	2979.7 (0.3)	7.0	10.8	66.8 (4.0)
2:1 BMOV/Tf	2968.0 (0.3)	2979.0 (0.4)	7.2	10.8	62.2 (2.8)

<sup>a</sup> Numbers in brackets correspond to standard deviation, over three experiments. <sup>b</sup> Expressed as full width at half magnitude. <sup>c</sup> Calculated as the peak area of B divided by the peak area of A of the  $-5/2$  signal.

calculated based on the peak areas of the Gaussian peaks fitted to the spectra. Peak area was preferred over peak height as (i) the peaks were partially overlapping and (ii) the calculated values obtained for peak widths (reported as full width at half magnitude) were slightly variable ( $\pm 1$  G), particularly for the  $-7/2_{||}$  peaks, across all samples, which is a result of glass-induced strain. This strain resulted in irregular broadening of the observed peaks and consequent reduction in the observed peak heights. Peak area would not be severely affected by this source of error. We also base our analysis on results obtained from the  $-5/2_{||}$  peak only as this peak yielded much more consistent results between experiments.

The Gaussian fitting of the four peaks of a representative experiment is presented in Figure 3, with the extracted parameters, averaged from three separate experiments, listed in Table 1. As shown in the table, the resonant field positions of the four peaks in each spectrum are identical. The relative intensities of the B conformation  $-5/2_{||}$  peaks (at 2968 G) in relation to that of the A conformation peaks (2979 G) are very similar. Under these conditions (0.05 M HEPES, pH 7.4, 0.16 M NaCl),  $VOSO_4$  strongly prefers the A conformation by about 5:3 (63–66% B relative to A) below 1 equiv; this preference is increased slightly upon addition of the second equivalent (52%). A similar pattern is observed with BMOV, with BMOV binding in a slightly lower proportion of B below 1 equiv of BMOV (67%) than with 2 equiv of BMOV present (62%), relative to A peak intensity. It should be noted that accurate fitting of the 2:1 BMOV/Tf spectrum required the introduction of a third set of Gaussian peaks, whose resonant field position corresponds exactly to BMOV. These peaks account for only 5% of the total area of the  $-5/2$  peaks but indicate that a small amount of free BMOV exists at the saturation limit of the protein. This residual BMOV provides further evidence that the intensities of the A and B conformations observed in vanadyl binding to apo-Tf need not be in a 1:1 ratio,<sup>42</sup> confirming the earlier results of White et al.<sup>30</sup>

Summarizing the results thus far, the room temperature EPR spectra of the VO-Tf and BMOV-Tf 1:1 and 2:1 solutions are identical, suggesting similar, if not identical, reaction products in which vanadyl ions bind in both A and B conformations in Tf. The interaction of BMOV with apo-Tf is

(42) We do not expect to observe a 1:1 ratio in the A and B conformations as the binding conformations were previously shown by Chasteen and co-workers to be pH, buffer, and anion dependent.<sup>29</sup> It was previously demonstrated that as the pH is raised to 10.0, the peaks in the EPR spectrum corresponding to the A conformation disappear and only the  $B_1$  and  $B_2$  resonances, in a 1:1 ratio, are observed by Q-band EPR spectroscopy. This result is in contrast to Fe binding, in which the A and B conformations correspond to Fe bound at the C- and N-terminus binding sites, respectively (see: Harris, D. C.; Aisen, P. In *Iron Carriers and Iron Proteins*; Loehr, T. M., Ed.; VCH Publishers: New York, 1989; Vol. 5, pp 239–342).

(41) Gerard, C.; Hugel, R. *J. Chem. Res.* **1980**, 314.

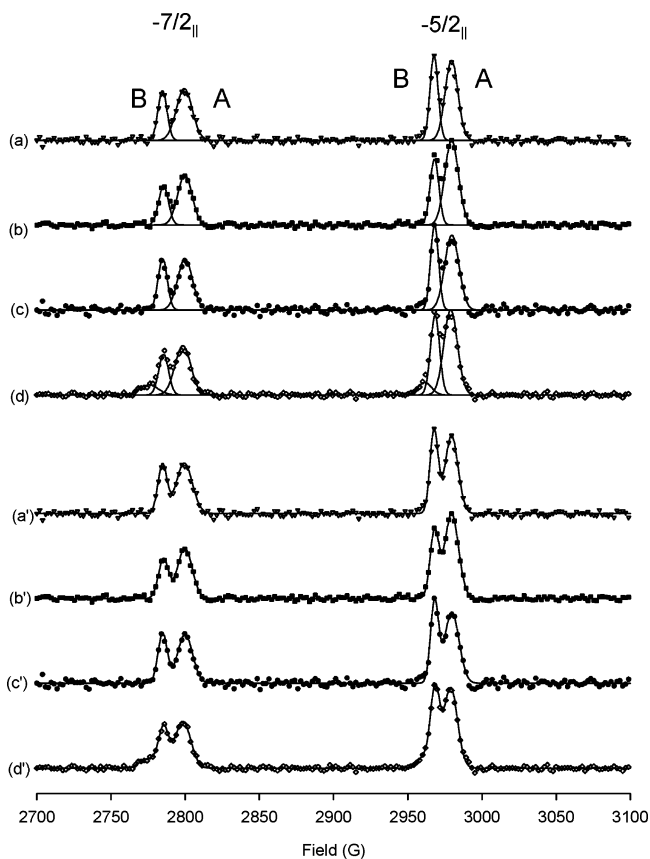


**Figure 3.** EPR spectra and Gaussian fitting (Table 1) of  $-7/2$  (downfield) and  $-5/2$  (upfield) parallel peak region of  $\text{VOSO}_4$  or BMOV and apo-Tf ( $T = 130$  K, pH 7.40, 0.16 M NaCl, 2700–3100 G, resolution 2048,  $\nu = 9.3450$  GHz) (a)  $[\text{VOSO}_4]/[\text{apo-Tf}] = 0.9$ ; (b)  $[\text{VOSO}_4]/[\text{apo-Tf}] = 1.8$ ; (c)  $[\text{BMOV}]/[\text{apo-Tf}] = 0.85$ ; (d)  $[\text{BMOV}]/[\text{apo-Tf}] = 1.9$ ; (a'–d') sum total of individual Gaussian peaks to yield fitted spectrum. For ease of viewing, every fourth data point is plotted, and the peaks corresponding to the A and B conformations are labeled.

specific, as evinced by the displacement of the bound  $\text{VO}^{2+}$  ions by Fe(III) ions and the absence of EPR signals from adventitiously bound vanadyl ions. The binding of vanadyl to apo-Tf does require a synergistic binding anion, and maltolate cannot facilitate binding of  $\text{VO}^{2+}$  to the Fe(III) binding sites. Further, chelation of the vanadyl ion does not induce any differences in the proportion of the two binding conformations (A or B, compared to  $\text{VOSO}_4$ ) when binding to apo-transferrin. All of these results taken together strongly suggest that BMOV is demetalated before vanadyl binds to apo-Tf. Since BMOV has been shown to possess a high thermodynamic stability ( $\log \beta_2 = 16.3$ )<sup>34</sup> apo-Tf must possess at least an equivalent affinity for  $\text{VO}^{2+}$  ions to be able to demetalate the BMOV complex at comparable concentrations.

#### Interactions of $\text{VOSO}_4$ and BMOV with Serum Albumin.

EPR spectra also demonstrate binding of vanadyl ions to HSA; those shown in Figure 4 are consistent with earlier results.<sup>33</sup> A comparison of the room temperature EPR spectra of 1:1  $\text{VOSO}_4/\text{HSA}$  and 1:1 BMOV/HSA solutions reveals subtle differences in resonant field positions and peak intensities. At room temperature, it appears that some BMOV still remains in solution as the 1:1 BMOV/HSA spectrum appears to be more isotropic than that obtained with  $\text{VOSO}_4$ .

Reactivity differences between BMOV and  $\text{VOSO}_4$  with HSA are more readily apparent in frozen solution EPR spectra (Figure

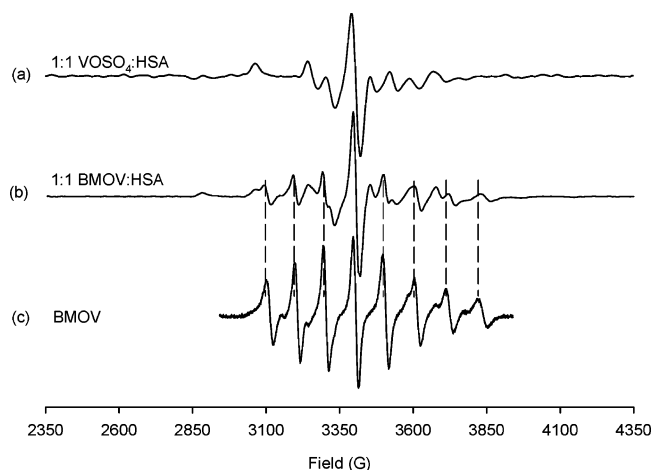


**Figure 4.** EPR spectra of VO–HSA ( $T = 298$  K, pH 7.4, 0.16 M NaCl,  $\nu = 9.5759$  GHz) (a)  $[\text{VO}^{2+}] = 0.285$  mM,  $[\text{HSA}] = 0.274$  mM; (b)  $[\text{BMOV}] = 0.502$  mM,  $[\text{HSA}] = 0.521$  mM; (c)  $[\text{BMOV}] = 1.22$  mM. Dashed lines indicate the resonant field positions of the nearly isotropic BMOV spectrum.

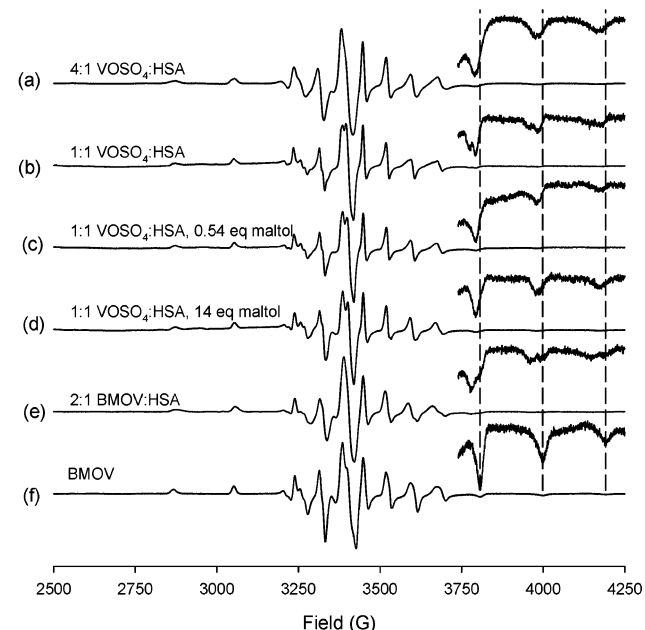


**Figure 5.** EPR spectra of  $\text{VOSO}_4$  or BMOV with HSA ( $T = 130$  K, pH 7.40, 0.16 M NaCl,  $\nu = 9.5786$  GHz); (a)  $[\text{VOSO}_4] = 2.18$  mM,  $[\text{HSA}] = 0.524$  mM; (b)  $[\text{VOSO}_4] = 0.40$  mM,  $[\text{HSA}] = 0.46$  mM; (c)  $[\text{VOSO}_4] = 0.37$  mM,  $[\text{HSA}] = 0.42$  mM,  $[\text{ma}] = 0.20$  mM; (d)  $[\text{VOSO}_4] = 0.37$  mM,  $[\text{HSA}] = 0.42$  mM,  $[\text{ma}] = 5.2$  mM; (e)  $[\text{BMOV}] = 0.485$  mM,  $[\text{HSA}] = 0.280$  mM; (f)  $[\text{BMOV}] = 1.02$  mM. Dashed lines indicate the resonant field positions of the high field parallel peaks of BMOV.

5) due to  $g$  and A anisotropy observed in the low temperature spectrum, which greatly increases the ability to identify and characterize different species within and between the samples. The interaction of BMOV with serum albumin does appear to result in slightly different reaction products. Coordination of  $\text{VO}^{2+}$  ions to the two distinct binding sites is exhibited by the top two spectra. Figure 5a shows the EPR spectrum of a 4:1 solution of  $\text{VOSO}_4$  and HSA and, therefore, is composed predominately of vanadyl ions bound nonspecifically to the weak sites. Contained within these broad peaks are the strong (Cu(II)) site signals, which are resolved in Figure 5b (1:1 solution of  $\text{VOSO}_4$  and HSA). The high field parallel resonances of Figure 5b each contain two peaks, one of which corresponds to the



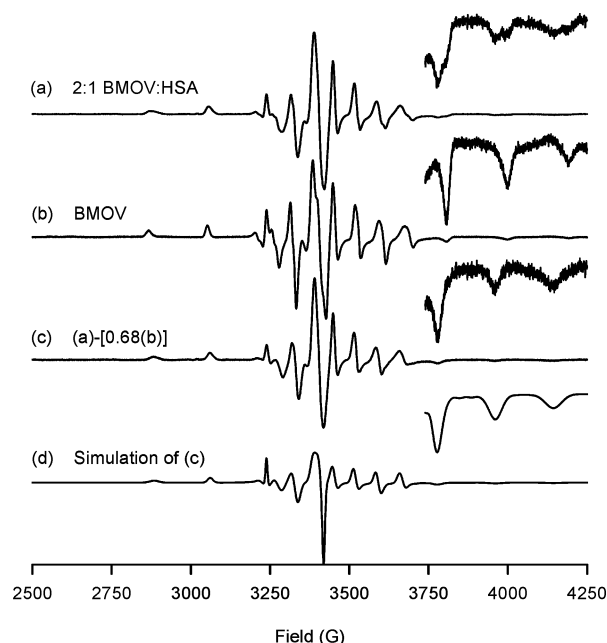


**Figure 6.** EPR spectra ( $T = 130$  K, pH 7.40, 0.16 M NaCl,  $\nu = 9.5786$  GHz) of (a) BMOV and HSA, [BMOV] = 0.512 mM, [HSA] = 0.280 mM; (b) BMOV alone, [BMOV] = 1.02 mM; (c) Subtraction of  $(0.68) \times b$  from a yields the EPR spectrum of the BMOV–HSA adduct; (d) Computer simulation of the EPR spectrum of BMOV–HSA.

nonspecifically bound  $\text{VO}^{2+}$  ions observed in Figure 5a. These results are entirely consistent with earlier studies.<sup>33</sup> Titration of maltol into that same solution yields spectra 5c and 5d (0.5 and 14 equivalents of maltol over  $\text{VO}_4/\text{HSA}$ , respectively). Addition of the strongly chelating ligand results in a decrease in intensity of the peaks corresponding to  $\text{VO}^{2+}$  bound at the strong site, with a concomitant increase in the weak site peak intensities. Since it is not thermodynamically possible for the vanadyl ion to spontaneously move from the strong site to the weak nonspecific sites, this maltol-induced change in the EPR spectrum represents formation of a new complex which we assign as a ternary maltol–VO–HSA species. The EPR spectrum of the ternary complex is very similar to that of  $\text{VO}^{2+}$  bound at the weak site; however this ternary species most likely represents the binding of a single maltol ligand to the  $\text{VO}^{2+}$  ion at the strong site. Due to the overlapping features in Figure 5c and 5d, we cannot discern whether vanadyl ions originally bound at the weak sites (Figure 5b) do in fact move to the strong site to produce more of the ternary complex. Maltol coordination to  $\text{VO}^{2+}$  at the strong site appears to be strong, as addition of 0.5 equiv of maltol results in a near complete depletion of the strong site  $\text{VO}^{2+}$  resonances (Figure 5c). No changes are observed in the EPR spectrum upon addition of 2, 5 (data not shown), or 14 equiv (Figure 5d) of maltol. Addition of excess maltol, however, does not lead to production of BMOV or the subsequent formation of the BMOV–HSA adduct (see below, Figure 6c) through an equilibrium process. Three dashed lines in the figure correspond to the high field peaks of BMOV (Figure 5f); even at a large excess of maltol, BMOV formation is not highly favored.

One of two processes can take place. The first possibility is that a single maltol binds to the vanadyl ion at the strong site, which changes the EPR spectrum to look much more like that of a vanadyl ion bound at a nonspecific weak site. The binding of two maltols can be discounted, as this would likely produce

the BMOV–HSA adduct, which we clearly demonstrate has a unique EPR spectrum (vide infra). The alternative process is that maltol reacts with  $\text{VO}^{2+}$  at the weak site to produce the ternary complex. Binding of maltol in this fashion does not cause a change in the EPR spectrum of weak site  $\text{VO}^{2+}$ . The stability of this complex is higher than that of strong site bound  $\text{VO}^{2+}$ , and by an equilibrium process this vanadyl fraction moves to the weak sites to form the ternary complex quantitatively.

Thus, the stability of this proposed ternary interaction is sufficiently high to successfully compete with BMOV formation ( $\log \beta_2 = 16.3$ ),<sup>34</sup> or other mechanisms are operative that prevent re-formation of BMOV. The addition of a significant excess of maltol appears to stabilize the interactions of the  $\text{VO}^{2+}$  ions with HSA through coordination, forming a ternary complex probably at the strong Cu(II) binding site as this would likely correspond to the most stable complex. Further discussion of this species is found below, in which we refer to the maltol–VO–HSA species as the ternary complex.

Addition of BMOV to HSA yields different reaction products. The EPR spectrum shown in Figure 5e corresponds to a 2:1 BMOV/HSA solution. In this spectrum, resonances (dashed lines) corresponding to intact BMOV are plainly visible, while a second set of resonances corresponds closely to that from strong site bound VO–HSA (downfield peaks, Figure 5b). Therefore, addition of BMOV to HSA results in a  $\text{VO}^{2+}$  species bound at the Cu(II) site, a vanadyl species that is most probably the intact BMOV complex (vide infra), thus forming an adduct. Secondly, BMOV does not appear to bind at the nonspecific weak sites at all. Weak site resonances (or ternary complex resonances), appearing in Figure 5a–d, are absent in Figure 5e. This second species, tentatively BMOV–HSA, will be referred to as the adduct complex.

Subtraction<sup>43</sup> of the EPR spectrum of BMOV (Figure 6b) from Figure 6a produces the EPR spectrum corresponding to BMOV bound at the Cu(II) (strong) site of HSA (Figure 6c). Computer simulation of Figure 6c with an orthorhombic spin Hamiltonian and the parameters listed in Table 2 yields the spectrum shown in Figure 6d. The spin Hamiltonian parameters obtained from the simulation were then compared to both strong and weak site bound VO–HSA, as well as a model system to fully characterize the interaction of BMOV with HSA (spin Hamiltonian parameters from all simulations are given in Table 2). Lastly, using spectrum 6b, we simulated the strong and weak binding site resonances for comparison to that of BMOV–HSA (simulations appear in Supporting Information, Figure S2). Due to a lack of discernible features in the perpendicular region that could be assigned to vanadyl ions in the strong site, only the parallel peaks were fitted (Table 2).

Order of addition of reactants is therefore of great importance to the VO/maltol/HSA system. Provision of  $\text{VO}^{2+}$  as a maltol complex (BMOV) to HSA yields a different reaction product than addition of the three components separately. If maltol is added to a solution of  $\text{VO}^{2+}$  and HSA, 1 equiv of maltol binds

(43) The proportion (0.68) of Figure 6b subtracted from Figure 6a to produce Figure 6c was determined by an iterative trial and error process in which the intensity of the BMOV resonances ( $B = 3804$  G, 3998 G and 4189 G) was reduced to zero. Careful examination of the resulting spectrum (and its inset) shows that the line shapes of all of the parallel resonances are Gaussian and there are no artifacts, at least in the parallel region, introduced by the subtraction. The value of 0.68 has not been corrected for differences in  $[\text{VO}^{2+}]$  between the two samples and is not indicative of the proportion of BMOV in the sample.



**Table 2.** Spin Hamiltonian Parameters<sup>a</sup> for Vanadyl–HSA Complexes, BMOV, and BMOV–Ligand Adducts (pH 7.4, 0.16 M NaCl)

complex	$g_z^a$	$g_x^a$	$g_y^a$	$g_{av}$	$\Delta g^b$	rhombicity <sup>b</sup>	$A_z^{a,c}$	$A_x^{a,c}$	$A_y^{a,c}$
VO–HSA strong	1.9265	1.9628 <sup>c</sup>	1.9600 <sup>c</sup>	1.9498	0.0525	1.0836	–166.50	–61.70 <sup>c,d</sup>	–55.48 <sup>c,d</sup>
VO–HSA weak	1.9355	1.9628 <sup>c</sup>	1.9600 <sup>c</sup>	1.9527	0.0496	1.1143	–164.50	–61.70 <sup>c,d</sup>	–55.48 <sup>c,d</sup>
BMOV–HSA	1.946	1.98	1.977	1.9676	0.0347	1.0968	–163.20	–59.00	–54.00
BMOV	1.938	1.979	1.975	1.9640	0.0383	1.1081	–171.00	–62.30	–65.00
BMOV–ImMe	1.944	1.980	1.977	1.9670	0.0353	1.0909	–164.80	–60.00	–55.50
BMOV–py <sup>e</sup>	1.9440	1.9790	1.9770	1.9766	0.0257	1.0606	–165.00	–58.90	–56.30

<sup>a</sup> Spin Hamiltonian parameters were obtained from computer simulation studies using the XSophe-Sophe-XeprView computer simulation software suite.<sup>36–38</sup> Error in  $g$ -values is  $\pm 0.001$  or  $\pm 0.0005$ ; error in  $A$  is  $\pm 0.5 \times 10^{-4} \text{ cm}^{-1}$ .  $T = 130 \text{ K}$ ; <sup>b</sup>  $\Delta g$  ( $g_z - g_{av}$ ) and rhombicity [ $(g_z - g_x)/(g_z - g_y)$ ] parameters are provided to allow comparisons between signals. <sup>c</sup> Units for vanadium hyperfine coupling are  $\times 10^{-4} \text{ cm}^{-1}$ . <sup>d</sup> Due to a lack of unique features in the perpendicular peaks, the simulated parameters for this region were fixed for VO–HSA strong and weak. <sup>e</sup> py = pyridine.<sup>44</sup>

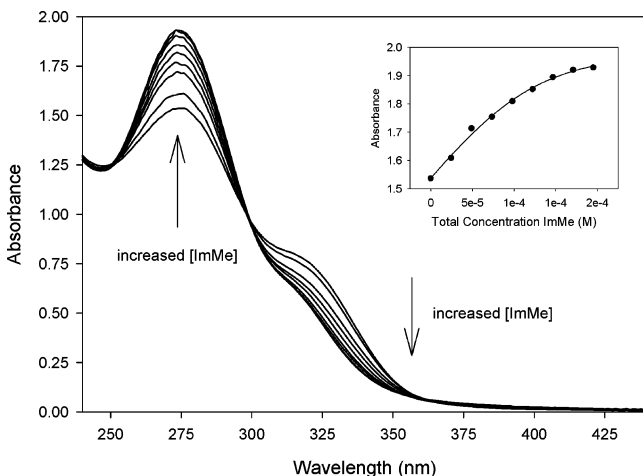


**Figure 7.** (a) Titration of BMOV (0.122 mM,  $V_0 = 25.5 \text{ mL}$ ) with ImMe (25.1 mM) monitored by electronic absorption spectroscopy, from 0 (initial titrant volume =  $0 \mu\text{L}$ ) to 1.6 molar equiv of ImMe (final titrant volume =  $200 \mu\text{L}$ ) ( $V_0 = 25.5 \text{ mL}$ ,  $T = 298 \text{ K}$ , pH 7.40, 0.16 M NaCl); (Inset) calculated (solid line) versus experimental absorbance (data points) values for the determination of  $\log K_1$  for the interaction of ImMe with BMOV ( $\lambda = 275 \text{ nm}$ ).

to the protein-bound vanadyl ions to form a ternary complex. This complex is highly stable to addition of a second maltol moiety. Reformation of BMOV appears to be inhibited in some way, preventing formation of the BMOV–HSA adduct or BMOV itself from vanadyl ions bound at the strong site. We later discuss possible mitigating factors leading to this behavior.

**Interaction of Imidazoles with BMOV.** BMOV binding to the Cu(II) binding site of HSA was modeled directly by interaction with 1-methylimidazole. The Cu(II) (strong) binding site of HSA is composed of a histidine (H3), two peptide nitrogens, and the free amine of the N-terminus. Vanadyl binding is thought to involve the histidine residue.<sup>33</sup> 1-Methylimidazole (ImMe) was used in the place of histidine to preclude potential metal binding at the carboxylic and free amine groups of the amino acid. Solution interactions of 1-methylimidazole with BMOV were studied by electronic absorption and EPR spectroscopy.

The equilibrium between 1-methylimidazole and BMOV was studied by electronic absorption spectroscopy. Titration of a solution of BMOV with ImMe (Figure 7) resulted in an increase in absorbance at 275 nm, with a broad decrease observed at  $\sim 325 \text{ nm}$ . Two clear isosbestic points at 252 and 297 nm were observed, indicating an equilibrium governing BMOV–ImMe adduct formation. Extinction coefficients for BMOV, ImMe and BMOV–ImMe were determined by Beer’s Law plots. For the adduct, large molar excesses ( $>25$ ) of ImMe were added to solutions of BMOV and the absorbance measured for several

different BMOV concentrations. An average of these values yielded an experimental  $\epsilon$  (275 nm) =  $(17.3 \pm 0.7) \times 10^3 \text{ M}^{-1} \text{ cm}^{-1}$  for the 1:1 adduct, compared to a value of  $(14.3 \pm 0.3) \times 10^3 \text{ M}^{-1} \text{ cm}^{-1}$  for the extinction coefficient of BMOV. ImMe itself has negligible ( $\epsilon_{\text{ImMe}} < 3 \text{ M}^{-1} \text{ cm}^{-1}$ ) absorbance at 275 nm.

Least-squares curve fitting analysis was applied to the absorbance data to obtain a value for the stability constant ( $\log K_1$ ) for adduct formation between ImMe and BMOV. The fit of the theoretical absorbance data to the experimental values is shown as an inset of Figure 7. To further improve the fit, the extinction coefficient for the adduct was allowed to vary from the experimental value; however, the average over three determinations correlated very well (the calculated result was  $(16.9 \pm 1.2) \times 10^3 \text{ M}^{-1} \text{ cm}^{-1}$ , within experimental error) to the independently determined extinction coefficient. The stability constant of the BMOV–ImMe adduct was found to be  $\log K_1 = 4.5 \pm 0.1$  ( $n = 3$ ), demonstrating that BMOV–protein interactions via exposed imidazoles are quite thermodynamically favorable and a viable route through which BMOV–HSA adducts could be formed.

EPR spectra of BMOV and BMOV–ImMe recorded at ambient temperature in aqueous solution are virtually identical ((BMOV)  $g_{\text{iso}} = 1.966(2)$ ,  $A_{\text{iso}} = -95.5(2) \times 10^{-4} \text{ cm}^{-1}$ ; (BMOV–ImMe)  $g_{\text{iso}} = 1.967(2)$ ,  $A_{\text{iso}} = -92.2(2) \times 10^{-4} \text{ cm}^{-1}$ ) with only a very slight reduction in  $A_{\text{iso}}$  and an insignificant increase in the isotropic  $g$  value. In  $\text{CHCl}_3$ , only a small change in the isotropic hyperfine coupling was observed ( $A_{\text{iso}} = -90.05 \times 10^{-4} \text{ cm}^{-1}$  for BMOV versus  $-90.40 \times 10^{-4} \text{ cm}^{-1}$  for BMOV–ImMe). The value of  $g_{\text{iso}}$  in  $\text{CHCl}_3$  was virtually unchanged. In general, the binding of the imidazole moiety broadens lines and changes isotropic  $g$  and  $A$  values slightly, compared to those for BMOV. An increase of nearly 2 G at  $\nu = 9.6002 \text{ GHz}$  was observed in the line width at half-height of the integrated  $-7/2$  parallel resonance (BMOV, 30.6 G; BMOV–ImMe, 32.4 G). It is also possible that the equilibrium position between cis and trans isomers has been shifted upon coordination of ImMe and/or an equilibrium between the associated and dissociated species is occurring, but the individual species cannot be resolved in the spectrum. Frozen aqueous solution spectra demonstrate a decrease in the  $A_z$  hyperfine coupling constant (Figure S3). Spin Hamiltonian parameters for BMOV and BMOV–ImMe in aqueous solution and 33% glycerol/water are shown in Table 2. The  $g$  and  $A$  matrices for frozen solutions are similar to those observed for the interaction of pyridine with BMOV.<sup>44</sup> In general, strong donor groups cause a decrease in the observed  $A$  values:  $|A_z|$  below  $170 \times 10^{-4}$

(44) Hanson, G. R.; Sun, Y.; Orvig, C. *Inorg. Chem.* **1996**, *35*, 6507–6512.

$\text{cm}^{-1}$  and  $|A_{x,y}|$  below  $60 \times 10^{-4} \text{ cm}^{-1}$  compared to the BMOV spectrum, consistent with previous observations.<sup>45</sup> The decrease in the  $A_z$  hyperfine coupling constant, together with an increase in the  $g_z$  value, is consistent with the addition of a nitrogen donor in the equatorial plane.<sup>39</sup> BMOV in solution predominantly adopts the cis conformation;<sup>44</sup> addition of an imidazole N-donor to the equatorial coordination sphere (assuming the imidazole binds with its ring parallel to the V=O bond) would expel the solvent water and decrease the  $A_z$  value by  $(4.2-7.3) \times 10^{-4} \text{ cm}^{-1}$ ,<sup>46</sup> which is close to what is observed. The increase in line width may be due to unresolved  $^{14}\text{N}$  superhyperfine coupling. Equatorial binding of pyridine to BMOV in chloroform and neat solution was previously explored by us.<sup>44</sup> Comparison of the spin Hamiltonian parameters of BMOV–ImMe with those of BMOV–HSA from Figure 6 shows that they are very similar, suggesting that BMOV is bound to a histidine of HSA, possibly H3. In particular, the  $\Delta g$  and rhombicity values reported in Table 2 are remarkably similar between the two species ( $\Delta g = 0.0347$  and  $0.0353$ ; rhombicity =  $1.0968$  and  $1.0909$  for BMOV–HSA and BMOV–ImMe, respectively). In turn, these values do not deviate much from the values found for BMOV, suggesting that BMOV interacts with both protein and ligand as the intact complex. Hyperfine coupling values, particularly  $A_z$ , also support the applicability of BMOV–ImMe as a model of the BMOV–HSA system.

## Discussion

The interaction of pharmaceuticals with serum proteins (e.g., Tf and HSA) is an important aspect of drug metabolism, capable of strongly affecting the distribution, biotransformation, and ultimately the mechanism of action. Current understanding of the pharmacological action of vanadium complexes is hampered by a lack of knowledge of the processes occurring before the active species reaches the putative active site. Indeed, the “true” active form of vanadium pharmaceuticals is the subject of much debate.<sup>17,40</sup> Thus, delineation of transport and biotransformation functions is important to provide insight into the chemical form of the vanadium species that ultimately leads to its antidiabetic effects.

**Interactions with apo-Transferrin.** The vanadyl–protein adduct produced through reaction of apo-Tf with BMOV was shown to be spectroscopically identical to that obtained with  $\text{VOSO}_4$ . In the case of BMOV, the protein is capable of binding 2 equiv of the BMOV complex, producing a  $(\text{VO})_2$ –Tf species in which the vanadyl ions occupy both Fe(III) binding sites. If any BMOV were to arrive in the bloodstream as the intact complex, free apo-Tf binding sites would rapidly induce complex decomposition with concomitant free ligand release. In result, this would then be indistinguishable from the situation of BMOV dissociating rapidly during the absorption process. Whereas the concentration of transferrin in the bloodstream is  $\sim 37 \mu\text{M}$ ,<sup>47</sup> the metal binding sites are generally only 30% occupied by Fe(III), leaving a significant metal binding reservoir ( $\sim 50 \mu\text{M}$ ) available for reaction with metal-based drugs. Such a reaction involving BMOV serves to highlight the importance of using a nontoxic ligand (such as FDA-approved maltol or ethylmaltol) in potential vanadium pharmaceuticals.

We have demonstrated that an endogenous chelating agent is fully capable of causing decomposition of an administered vanadyl complex. Apo-Tf is therefore a viable transport mechanism for vanadyl ions sourced from either inorganic ( $\text{VOSO}_4$ ) or chelated sources (BMOV). Importantly, binding of both  $\text{VO}^{2+}$  and BMOV to the Fe(III) binding sites in apo-Tf required the presence of (bi)carbonate, and EPR spectra revealed little preference for the A or B conformation relative to  $\text{VOSO}_4$ . Lastly, maltolate was found to be incapable of acting as a synergistic anion in binding of BMOV to apo-Tf.

Since the spectra presented for both BMOV and  $\text{VOSO}_4$  with apo-Tf are virtually identical, the metal–protein complexes derived from both vanadyl sources must be the same. This result is inconsistent, however, with data recently reported by other researchers,<sup>40</sup> interpreted as indicating that the reaction products resulting from the interactions of  $\text{VOSO}_4$  or BMOV with apo-Tf are different. Simulation data and frozen solution spectra, reported herein, tend to refute this conclusion. A close examination of the previously reported room temperature BMOV–HTf EPR spectrum<sup>40</sup> indeed reveals the presence of two components. The first component is isotropic, and the resonant field positions are identical to those observed for BMOV (assuming the spectra were measured at similar microwave frequencies). The second component has a spectrum similar to that shown herein as Figure 1b. In addition, the EPR spectrum of  $\text{VOSO}_4$ –HTf is neither rigid limit nor isotropic, but more typical of molecules tumbling in the slow motion regime; consequently measurement of  $A_{\text{iso}}$  from the apparent isotropic resonances is invalid.

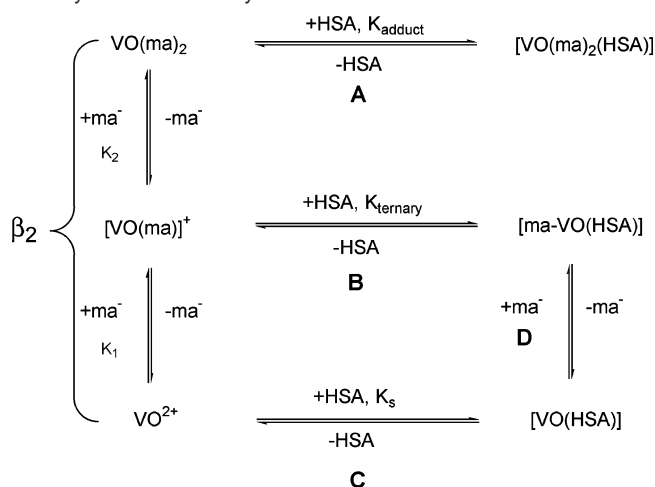
As noted above, our data support strongly the formation of identical VO–transferrin complexes from either BMOV or  $\text{VOSO}_4$ ; hence, interactions with this serum protein would result in the delivery of identical VO metabolites to target tissue for both chelated and free vanadium(IV) sources. This similarity in reactivity with apo-transferrin shared between BMOV and  $\text{VOSO}_4$  is contrasted by their interactions with human serum albumin (HSA).

**Interactions with Human Serum Albumin.** EPR spectra clearly demonstrate different modes of reactivity for the two vanadyl sources, seemingly in agreement with previous findings.<sup>40</sup> In this study however we have expanded upon earlier results and characterized these differences in far greater detail. Willsky et al. suggested that perhaps a ternary maltolate–vanadyl–albumin complex formed, but beyond comparison of room-temperature EPR spectra, no analysis of the reaction products was given. Frozen solution EPR spectra reported herein demonstrate that two different species (the adduct BMOV–HSA, i.e.,  $[\text{VO}(\text{ma})_2(\text{HSA})]$ ) and the ternary complex  $[\text{ma}-\text{O}(\text{HSA})]$  can be formed in the vanadyl–maltol–HSA system. Scheme 1 indicates the possible pathways for production of these species and indeed represents a complete description of the VO–ma–HSA system consistent with our experimental results. The reaction of BMOV and HSA leads to the formation of the BMOV–HSA adduct complex through binding of an intact BMOV molecule at the sixth coordination position (path A,  $K_{\text{adduct}}$ ). It does not seem possible to produce BMOV or the BMOV–HSA adduct from the ternary maltol–VO–HSA complex through addition of excess maltol. The ternary complex with different EPR parameters can be formed by titrating VO–HSA (formed via path C) with maltol. Reaction path D details the course of such a reaction. Thermodynamically, paths B and

(45) Smith, T. S., II; LoBrutto, R.; Pecoraro, V. L. *Coord. Chem. Rev.* **2002**, *228*, 1–18.

(46) Smith, T. S., II; Root, C. A.; Kampf, J. W.; Rasmussen, P. G.; Pecoraro, V. L. *J. Am. Chem. Soc.* **2000**, *122*, 767–775.

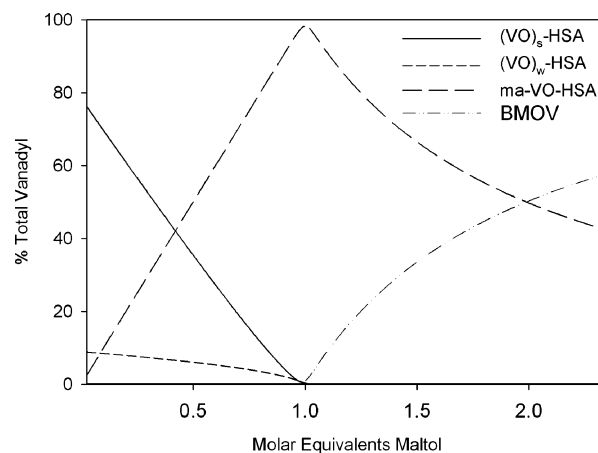
(47) Baker, E. N. *Adv. Inorg. Chem.* **1994**, *41*, 389–463.

**Scheme 1.** Chemical Equilibria Describing the Vanadyl–Maltol–HSA System

D should be equivalent, yielding the ternary maltol–VO–HSA complex governed by an overall stability constant  $\beta_{\text{ternary}}$ ; however, we have not tested this hypothesis as the  $[\text{VO}(\text{ma})]^+$  species does not exist at pH 7.4. The data suggest however that the two end products are not interchangeable; BMOV–HSA and maltol–VO–HSA do not appear to exist in equilibrium with each other because the corresponding EPR spectra do not show any evidence of the other species. Such an equilibrium would require association/dissociation of a maltol. We have demonstrated that re-formation of BMOV from the ternary complex is not favored, in that the ternary complex resists addition of a second maltol ligand (Figure 5).

Thermodynamic models of the solution chemistry indicate that *at least* ternary complex formation should take place for any interaction of BMOV-sourced  $\text{VO}^{2+}$  with HSA to take place. With BMOV as the vanadyl source, the high thermodynamic stability of BMOV precludes complete abstraction of the metal ion to the protein (Scheme 1, path C), in which the strong site binds with a stability several orders of magnitude lower than  $\log \beta_2$  of BMOV. While the EPR spectra do confirm the observation of Willsky et al. that the reaction products of BMOV and  $\text{VOSO}_4$  with HSA are different, the correct interpretation is that the presence of the chelating maltol ligands imparts site selectivity to the system, as the weak binding sites are not strong enough to abstract the metal ion from the BMOV chelate complex and, hence, BMOV binds to the protein as the intact complex (path A).

Stability constants for both strong and weak site binding of  $\text{VO}^{2+}$  cations by HSA have been defined previously,<sup>32,33</sup> and neither site binds  $\text{VO}^{2+}$  ions more strongly than do the two maltolato ligands. In a hypothetical solution of 1 equiv of vanadyl ion, 20 equiv of HSA, and 2 equiv of maltol at pH 7.4, 84% of the total  $\text{VO}^{2+}$  would be in the form of BMOV, according to our calculation. Experimentally, interaction of BMOV with HSA is observed at ratios far below 20:1, confirming that complete abstraction of the vanadyl ion from BMOV is not the reaction path. Surprisingly, two distinct reaction products are detected, depending on the source of vanadyl. Titration of a 1:1 solution of  $\text{VO}^{2+}$  and HSA with maltol demonstrates that these two products are not readily interchangeable; perhaps the equilibrium to produce BMOV–HSA is very slow from the ternary complex, possibly due to

**Figure 8.** Titration simulation of a 1:1 solution of  $\text{VO}^{2+}$  and HSA ( $[\text{VO}^{2+}] = [\text{HSA}] = 0.01 \text{ mM}$ ;  $\log \beta_{\text{ternary}} = 15.0$ ).

slow conformation changes required of the protein for binding of the second maltol moiety to take place. A simulation of such a titration (Figure 8), with an arbitrary (and optimistic)  $\log \beta_{\text{ternary}} = 15.0$ , predicts ternary complex formation up to 1 equiv of maltol, followed by BMOV formation and a steady decrease in ternary complex concentration. Such a result is not supported by our data, indicating that either (i) ternary complex stability is much higher than BMOV stability or (ii) the system is dominated by kinetic factors which prevent re-formation of BMOV or the adduct complex. The stability of the ternary complex must be less, however, than that of the adduct, as addition of BMOV to HSA produces the adduct complex quantitatively, with no apparent production of the ternary complex. Thus, the observations strongly support binding of only one maltol to a vanadyl ion at the strong site. Neither binding of a second maltol nor production of BMOV and/or the BMOV–HSA adduct in the presence of excess maltol is feasible. It appears likely that this system is governed by other factors, possibly a slow protein folding step which protects the ternary complex from further reaction with maltol.

Previous studies of  $(\text{Fe})_2$ -transferrin<sup>47</sup> have demonstrated that purely thermodynamic arguments are not necessarily accurate predictors of metalloprotein chemistry with chelating ligands. Several studies have reported slow  $\text{Fe}(\text{III})$  release from  $(\text{Fe})_2$ -transferrin to chelators that, by thermodynamic arguments, should easily abstract the metal ion from the binding sites.<sup>48–52</sup> Frequently, the main limiting factor is a slow conformational change of the diferric protein to allow access to the metal ion by the chelating ligand. Further, the chemical form of Cu ions has been shown to strongly influence its interactions with HSA.<sup>53</sup> Presentation as the histidine chelate limits copper binding at nonspecific sites and promotes full loading of the  $\text{Cu}(\text{II})$  site at the N-terminus. Our results appear to mirror those obtained with Cu. The BMOV–ImMe interaction lends additional support to our characterization of the BMOV–HSA adduct interaction.

Imidazoles may cause dissociation of one of the maltolato ligands in addition to the cis/trans isomers described previously;

(48) Baldwin, D. A. *Biochim. Biophys. Acta* **1980**, 623, 183–198.(49) Cowart, R. E.; Swope, S.; Loh, T. T.; Chasteen, N. D.; Bates, G. W. *J. Biol. Chem.* **1986**, 261, 4607–4614.(50) Kretschmar, S. A.; Raymond, K. N. *Inorg. Chem.* **1988**, 27, 1436–1441.(51) Harris, W. R.; Bali, P. K. *Inorg. Chem.* **1988**, 27, 2687–2691.(52) Bali, P. K.; Harris, W. R.; Nasset-Tollefson, D. *Inorg. Chem.* **1991**, 30, 502–508.(53) Valko, M.; Morris, H.; Mazur, M.; Telsler, J.; McInnes, E. J. L.; Mabbs, F. E. *J. Phys. Chem. B* **1999**, 103, 5591–5597.



however, fitting of the electronic absorption data was not improved by including 1:1:1 or 1:1:2 VO/maltol/ImMe species in the model. Formation of a VO(acac)<sub>2</sub>–bovine serum albumin (BSA) complex has been observed;<sup>17</sup> the vanadyl complex appeared to remain intact in the adduct. The magnitude of the stability constant obtained suggests that adduct complex formation between imidazole functionalities and the free coordination position of BMOV and its analogues could be biologically significant. Previous studies of adduct formation between vanadium(IV) complexes have also determined significant thermodynamic stability for formation of adduct complexes. The coordinating ability of certain solvents to BMOV was found to be pyridine > water > methanol > dichloromethane.<sup>34</sup> Coordination of the sixth position ligand can be either cis or trans to the V=O bond,<sup>44</sup> but for strong donors such as pyridine the cis isomer is dominant.<sup>44,54–57</sup>

The interaction of pyridine with VO(acac)<sub>2</sub> in benzene has also been studied. A smaller log *K*<sub>1</sub> value of 1.89 at 18 °C was found.<sup>58</sup> In this study, however, the stability constant was determined in H<sub>2</sub>O, itself a competing ligand for the open coordination position of BMOV. The coordinating ability of ImMe would therefore likely be greater than that of pyridine. Earlier studies utilized conditions that would greatly favor ternary complex formation: formation of the adduct in neat solution<sup>34</sup> or in a noncoordinating (i.e., noncompeting) solvent system.<sup>44,58</sup> Thus, a histidine side chain could easily replace a water molecule in the sixth coordination site of BMOV under biological conditions. In the absence of direct spectroscopic evidence, it is possible that the complex formed between BMOV and HSA could in fact be a ternary complex, with the BMOV molecule tethered to the protein via the coordinating histidine residue in the Cu(II) binding site. Additionally, if BMOV arrives at the target tissue as the intact complex, this interaction could be one method by which BMOV-sourced vanadyl ions become bound by intracellular proteins, via nonspecific interactions with dangling histidine side chains accessible on protein surfaces and binding sites.

**Protein Binding of BMOV in Serum.** Despite this interesting reactivity difference between BMOV and VOSO<sub>4</sub>, the BMOV/HSA interaction may lose its importance in the *in vivo* environment, due to the presence of apo-Tf. Previous competition studies have shown that VO<sup>2+</sup> ions bind preferentially to apo-Tf over HSA,<sup>59</sup> and computer models of *in vivo* serum solutions also support the predominant role of apo-Tf for vanadyl ion transport.<sup>60</sup> Recent work from our laboratories indicates that at least a majority of labeled BEOV is decomposed upon entering the bloodstream.<sup>14</sup> This study provides evidence that apo-Tf may be one mechanism by which this demetalation takes place.

It is interesting to speculate, however, that while VOSO<sub>4</sub> associates preferentially to apo-Tf over HSA in competition

studies,<sup>59</sup> the provision of the vanadyl source as a chelate may in fact augment HSA binding to such a degree that the BMOV–HSA interaction could indeed be physiologically relevant. We are currently investigating this possibility. BMOV can bind as the intact complex to HSA, but it is unclear whether this adduct formation protects the complex from degradation by apo-Tf. It is clear from the EPR spectra that apo-Tf interacts strongly with BMOV, but ternary complex formation is not likely operative. Whether adduct formation between BMOV and HSA would allow for *in vivo* competition between the two proteins for VO<sup>2+</sup> coordination and transport remains to be elucidated. Previously, ESEEM evaluation of bone vanadium derived from orally administered BEOV clearly showed dissociation of the complex prior to bone uptake.<sup>61</sup> As bone may be a significant *in vivo* source of releasable vanadium for prolonged glucose-lowering effect, the effect of ternary BMOV HSA adduct formation most likely occurs prior to tissue deposition, as also concluded from potentiometric titration studies.<sup>60</sup> Strongly supporting this hypothesis are the recent crystal structures of two cytoplasmic phosphatases that were treated with BMOV. Both X-ray and NMR data demonstrated the presence of uncomplexed vanadate (VO<sub>4</sub><sup>3-</sup>) in the active sites of both enzymes,<sup>62</sup> providing further evidence for BMOV decomposition prior to incorporation into the presumed intracellular target molecules.

Extracellularly, provision of a chelated vanadyl source may in fact lead to an inadvertent targeting effect, in that the presence of the chelating ligand augments the binding ability of the endogenous albumin. Ternary/adduct complex formation with the original coordination sphere (i.e., two maltolato ligands) is not necessarily the situation in serum, where several low molecular weight bioligands (e.g., citrate, oxalate, nucleotides) are present. These bioligands can interact with BMOV to form VOAB (where A = maltolato and B = endogenous bioligand), some with significantly greater stability than BMOV alone.<sup>63</sup> These species could then go on to interact with HSA. Kiss et al. predicted that if the stability of VO–HSA binding was increased to ~1/6 that of apo-Tf, the proportion of vanadyl ions bound to HSA increases from 0 to 80%.<sup>60</sup> Obviously the solution modeling calculations did not take into account ternary and adduct complex formation discussed here, which would also serve to increase the HSA-bound fraction. Therefore, the BMOV–HSA adduct could possibly be an early active species leading to the augmented antidiabetic effects, consistent with predicted VO(acac)<sub>2</sub> adduct formation.<sup>17</sup>

One possible mechanism for this increased efficacy is that adduct formation with HSA protects the complex from oxidation. Pyridine adducts of BMOV have been shown to be highly stable to oxidation in solution,<sup>34</sup> while vanadyl–transferrin species are unstable and oxidize relatively rapidly to V(V).<sup>59</sup> Alternatively, if the transferrin pathway is dominant, metal binding by this protein may lead to more rapid cellular delivery in a manner parallel to Fe ingress into cells. Whether divanadyl–transferrin binds and activates the cellular transferrin receptor in the same way as does holotransferrin has not been shown. Another possible mechanism of an HSA effect is that HSA complexation slows transit of the vanadyl chelate to the target

(54) Atherton, N. M.; Gibbon, P. J.; Shohoji, M. C. B. *J. Chem. Soc., Dalton Trans.* **1982**, 2289–2290.

(55) Sawant, B. M.; Shroyer, A. L. W.; Eaton, G. R.; Eaton, S. S. *Inorg. Chem.* **1982**, *21*, 1093–1101.

(56) Yordanov, N. D.; Zdravkova, M. *Polyhedron* **1993**, *12*, 635–639.

(57) Da Silva, J. J. R. F.; Wootton, R. *J. Chem. Soc., Chem. Commun.* **1969**, 421–422.

(58) Walker, F. A.; Carlin, R. L.; Rieger, P. H. *J. Chem. Phys.* **1966**, *45*, 4181–4185.

(59) Chasteen, N. D.; Grady, J. K.; Holloway, C. E. *Inorg. Chem.* **1986**, *25*, 2754–2760.

(60) Kiss, T.; Kiss, E.; Garribba, E.; Sakurai, H. *J. Inorg. Biochem.* **2000**, *80*, 65–73.

(61) Dikanov, S. A.; Liboiron, B. D.; Thompson, K. H.; Vera, E.; Yuen, V. G.; McNeill, J. H.; Orvig, C. *J. Am. Chem. Soc.* **1999**, *121*, 11004–11005.

(62) Peters, K. G. et al. *J. Inorg. Biochem.* **2003**, *96*, 321–330.

(63) Kiss, T.; Kiss, E.; Micera, G.; Sanna, D. *Inorg. Chim. Acta* **1998**, *283*, 202–210.

tissues, similar to HSA binding of gadolinium-based pharmaceuticals increasing gadolinium residence time in blood.<sup>64</sup> This mechanism is also consistent with blood circulation monitoring studies in which vanadyl picolinate clears the bloodstream more slowly than vanadyl sulfate. Rapid clearance correlated with reduced in vivo efficacy for the latter.<sup>65</sup> Delayed blood circulation clearance, whether by ileal vs jejunal administration or by enteric-coated encapsulation, appears also to enhance in vivo efficacy of bis(6-methylpicolinato)oxovanadium(IV) or VOSO<sub>4</sub>, respectively.<sup>66,67</sup>

BMOV–HSA adduct formation may also slow renal excretion of administered vanadium or protect from metal ion abstraction by transferrin. Either mechanism would serve to increase the portion of the chelated vanadium dose that reaches the active site(s) over unprotected sources such as VOSO<sub>4</sub>. Suffice to say, both serum proteins interact with BMOV, and likely other chelated V(IV) sources as well. These interactions with chelated vanadyl sources could be of greater importance in determining pharmaceutical efficacy than previously realized.

### Conclusions

We have demonstrated that a chelated vanadium source will strongly interact with two common blood serum proteins, apo-transferrin and albumin. Reaction of BMOV with apo-transferrin can be expected to completely dissociate the complex, however, it may not be the dominant effect in delivery of vanadium from vanadyl chelates to target tissues. Reaction products formed by BMOV and VOSO<sub>4</sub> with albumin are not identical, and the presence of chelating ligands such as maltolate may in fact augment vanadium binding to this serum protein.

These results lead to a more complete picture of the transport and metabolism of vanadium pharmaceuticals. Interactions with apo-Tf, resulting in demetalation of the complex, favors a “ligand taxi” mechanism, in which the increased antidiabetic effects of chelated vs inorganic vanadium are simply the result of increased gastrointestinal absorbance. However, a thermodynamically favored reaction with albumin would tend to slow plasma clearance of chelated vanadium, augmenting the insulin-enhancing activity of these sources compared to vanadyl sulfate in a postabsorptive fashion. Thus, chelation may serve a dual purpose: increased lipophilicity to augment gastrointestinal absorption and facilitated formation of protein adducts with a greater stability than for uncomplexed vanadium. This leads to the intriguing possibility that adduct or ternary albumin complexes could be the pharmacologically active species, or at the very least the main method of vanadium delivery to cells. Competition studies to determine the distribution of BMOV between apo-Tf and HSA, currently underway, will be useful to delineate the true transport role of these proteins in vivo.

**Acknowledgment.** This research was supported by the Natural Sciences and Engineering Research Council of Canada, Canadian Institutes of Health Research, Kinetek Pharmaceuticals, Inc., the Science Council of British Columbia (B.D.L., GREAT program), the Swiss National Science Foundation (N.A.), and an Australian Research Council International Researcher Exchange (IREX) program grant to G.R.H. and C.O.

**Supporting Information Available:** Figures S1, S2, and S3, EPR spectra of BMOV–apo-Tf solutions, VOSO<sub>4</sub>–HSA solutions and computer simulations at 4:1 and 1:1 ratios, and frozen solution EPR spectra of BMOV and ImMe 2:1 solutions. This material is available free of charge via the Internet at <http://pubs.acs.org>.

JA043944N

- (64) Caravan, P.; Cloutier, N. J.; Greenfield, M. T.; McDermid, S. A.; Dunham, S. U.; Bulte, J. W. M.; Amedio, J. C., Jr. *J. Am. Chem. Soc.* **2002**, *124*, 3152–3162.
- (65) Yasui, H.; Takechi, K.; Sakurai, H. *J. Inorg. Biochem.* **2000**, *78*, 185–196.
- (66) Fugono, J.; Yasui, H.; Sakurai, H. *J. Pharm. Pharmacol.* **2001**, *53*, 1247–1255.
- (67) Fugono, J.; Yasui, H.; Sakurai, H. *J. Pharm. Pharmacol.* **2002**, *54*, 611–615.